Chemical Engineering Science Vol. 38, No. 1, pp. 29–43, 1983
Printed in Great Britain.

0009–2509/83/010029–15$03.00/0

AUTOCATALYTIC REACTIONS IN THE ISOTHERMAL, CONTINUOUS STIRRED TANK REACTOR

ISOLAS AND OTHER FORMS OF MULTISTABILITY

P. GRAY* and S. K. SCOTT
Department of Physical Chemistry, University of Leeds, Leeds LS2 9JT, England

(*Received* 2 *July* 1982)

Abstract—Autocatalytic reactions are often complicated, and analyses of their behaviour in open systems can seem too particular to permit useful generalisation. We study here the simplest of circumstances (uniform temperatures and concentrations in the isothermal CSTR) and the simplest of reaction schemes: (i) quadratic autocatalysis ($A+B\rightarrow 2B$); and (ii) cubic autocatalysis ($A+2B\rightarrow 3B$). The catalyst B may be stable or have a finite lifetime ($B\rightarrow$ inert products). Allowing for this finite lifetime adds another dimension to the interest.

The phenomena encountered include multistability, hysteresis, critical extinctions, critical ignitions, and anomalous relaxation times (though infinite values do not arise). Patterns of stationary states as function of residence time can show isolas and mushrooms. All these aspects yield to simple algebraic analysis. The presence of the catalyst B in the inflow can make qualitative differences of a kind parallelled by an additional, non-catalytic reaction of the same stoichiometry (e.g. $A\rightarrow B$). Invoking the reversibility of the reactions neither increases nor diminishes their variety, and thermodynamic considerations have little to do with the many different patterns of reactivity displayed.

The local stability of the various stationary states has also been characterized. Quadratic autocatalysis shows limited variety (stable node, stable focus); cubic autocatalysis generates all the kinds of stationary state possible in a two-variable system. Again all the algebra is straightforward if not always simple. Sustained oscillatory behavior (limit cycles) also occur.

All these remarks relate to isothermal systems, but there are the most striking parallels between isothermal autocatalysis and the exothermic, first-order reaction in the CSTR. Behaviour with an autocatalyst of complete stability corresponds to perfect heat insulation (adiabatic operation) in the non-isothermal, exothermic system.

INTRODUCTION

Few fields in fundamental chemical reactor engineering have been as intensively cultivated as studies of the single, irreversible exothermic reaction in the continuous stirred tank reactor (CSTR). Originally, interest centred on questions of unique vs multiple stationary states and on the phenomena of ignition, extinction and hysteresis. Later, attention was focussed on stability, local and global, and on the possibilities of sustained oscillatory behaviour. In the early years, combustion science and chemical reactor engineering sometimes rediscovered one another's ideas, and some of these overlaps are reviewed elsewhere[1]. In more recent times, the codifications of behaviour by Uppal, Ray and Poore[2, 3] offer authoritative surveys, although even these contain generalisations that have been modified or criticised[4, 5].

It is surprising but true that no such extensive studies have been made of the corresponding isothermal prototypes, where feedback is not thermal but autocatalytic; although preliminary investigations by Lin[6] have recently established ranges of multiplicity and the stability of different solutions for the basic autocatalytic ratelaws. This is despite great activity by inorganic solution chemists on the oscillatory Belousov–Zhabotinskii reaction, and by biochemists on enzyme systems. The result is that we know less about some of the simplest autocatalytic systems than about complicated special cases.

The simplicity of these systems leads to their algebraic analysis remaining tractable throughout. This in turn allows some striking physical insights into the causes of the various patterns: these clarifications allow us to test (and in some cases, to refute) some recent ideas which have gained ground. These include suggestions of infinitely long relaxation times[7] or "critical slowing-down". (We shall see that "slowing-down" occurs, but not in the interpretation used so far.) It has also been stated that isothermal systems cannot have extinction associated with increases in the residence time or ignition associated with decreases[8]. This is equivalent to excluding mushrooms from isothermal systems. We are also able to clarify the effect of reversibility: it is here that thermodynamics has its major influence on open systems.

Because oscillatory systems are of interest to chemists as well as chemical engineers we shall present some of the background to autocatalysis and open systems in Section 2. The main thrust of the present work is found in Sections 4 and 5, where we model in a very simple way the behaviour of real catalysts that can lose their activity (or be poisoned) or decay in time.

Strong analogies may be drawn between these systems and the non-isothermal reactions. Isothermal autoca-

*Author to whom correspondence should be addressed.

talysis with an unstable catalyst resembles non-isothermal, non-adiabatic behaviour; isothermal autocatalysis with a stable catalyst resembles non-isothermal reaction under adiabatic conditions.

2. STOICHIOMETRY, KINETICS AND MASS BALANCE FOR AUTOCATALYTIC REACTIONS IN OPEN SYSTEMS: FLOW DIAGRAMS

The simplest forms of autocatalytic reactions may be expressed by the prototype reaction-steps:

$$A + B \rightarrow 2B$$

$$A + 2B \rightarrow 3B.$$

The stoichiometry of these reactions is $A \rightarrow B$, but the reaction rate depends differently on the concentration of the product species B:

$$\text{rate} \quad \alpha[A][B]^n, \qquad n = 1,2.$$

We will refer to these cases as (i) quadratic or simple autocatalysis ($n = 1$) and (ii) cubic autocatalysis ($n = 2$).

In a closed system the rate of an autocatalytic reaction rises to a maximum, and then falls to zero as the final (equilibrium) state is achieved. This results in an *S*-shaped curve of product concentration vs time. These curves are typical of many biological cases, for example the growth of populations in the presence of a limited food supply and the spread of infectious diseases; and they also occur for many gas–solid reactions or solid–solid transitions where the rate is proportional to the surface area of contact between the two phases.

Autocatalysis in open systems

For the *simple* autocatalytic reaction ($n = 1$) the mass-balance equation in an open system is

$$\frac{db}{dt} = k\,a\,b - k_{res}b \tag{1}$$

where k is the reaction rate-constant and $k_{res} = 1/t_{res}$ is the inverse of the residence time, and plays the role of a first-order rate-constant. Implicit in eqn (1) is the assumption that the concentration of B in the inflow is zero ($b_0 = 0$).

It is convenient to non-dimensionalize the problem. There are two possible choices for the dimensionless extent of reaction γ

$$\gamma = \frac{a_0 - a}{a_0} \quad \text{or} \quad \gamma = \frac{b}{a_0}. \tag{2}$$

For the simple cases in this section these definitions are equivalent, because of the extra constraint

$$a + b = a_0. \tag{3}$$

This important condition expresses the fact that a and b cannot vary independently. There is only one variable in this problem.

In dimensionless terms equation (1) becomes

$$\frac{d\gamma}{d\tau} = 4\gamma(1 - \gamma) - \gamma/(Da). \tag{4}$$

The factor 4, in the first term on the r.h.s. of eqn (4), which represents the chemical rate of production of B, $(d\gamma/d\tau)_{chem}$, occurs so it rises to a maximum of unity. This normalization will be useful when comparing the different cases to be studied here. The group (Da) represents a dimensionless residence-time

$$(Da) = t_{res}/t_{chem}$$

and for the chemical time t_{chem} we shall choose

$$t_{chem} = \frac{\text{initial conc. of } A}{\text{maximum chemical reaction rate}}$$

$$= \frac{a_0}{\frac{1}{4}ka_0^2} = \frac{4}{ka_0}.$$

Hence

$$(Da) = \frac{1}{4}\,ka_0t_{res}$$

and

$$\tau = t/t_{chem} = \frac{1}{4}\,ka_0t$$

where τ is the dimensionless time.

The second term on the r.h.s. of eqn (4) represents the rate of outflow of B, $(d\gamma/d\tau)_{flow}$. This and the rate of production are plotted as functions of γ in Fig. 1(a). The production curve is zero at $\gamma = 0$ and 1, rising to a maximum at $\gamma = \frac{1}{2}$. The loss line is a straight line of gradient $1/(Da)$, and the intersections of the two curves represent the stationary-states, when $d\gamma/d\tau$ is zero.

Long residence-times, or slow flows correspond to loss lines with low slope. The gradient increases as the residence-time becomes shorter. For slow flow-rates such that $(Da) > (1/4)$, there are two intersections; one at $\gamma_1 = 0$ and one given by

$$\gamma_2 = 1 - \frac{1}{4}(Da)^{-1}.$$

Throughout this paper we will use the subscript 1 to refer to the lowest, positive (or zero) stationary-state solutions, and the subscripts 2 and 3 for other solutions in order of increasing γ.

As (Da) tends to (1/4), the two solutions converge at $\gamma_3 = 0$, and for faster flowrates, the non-zero intersection becomes negative and is not physically realistic. Thus the condition for multistability and for a positive, non-zero rate of reaction is

$$(Da) > \frac{1}{4} \quad \text{or} \quad t_{res} > 1/k\,a_0.$$

We may perform a similar analysis for the *cubic*

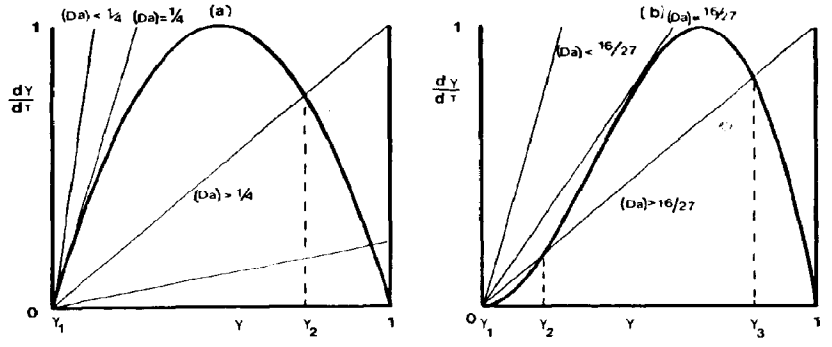

Fig. 1.

autocatalysis, for which the mass-balance equation is

$$\frac{db}{dt} = kab^2 - k_{res}b. \tag{5}$$

In dimensionless terms this becomes

$$\frac{d\gamma}{d\tau} = \frac{27}{4}(1-\gamma)\gamma^2 - \gamma/(Da) \tag{6}$$

where the normalizing factor 27/4 arises because the maximum of the production rate is 4/27, occurring when $\gamma = 2/3$. The chemical time, on which (Da) and τ are based, also contains this factor

$$t_{chem} = a_0 \Big/ \left(\frac{4}{27} k a_0^3\right)$$

hence

$$(Da) = \frac{4}{27} k a_0^2 t_{res}; \quad \tau = \frac{4}{27} k a_0^2 t.$$

The cubic rate of production curve, plotted as a function of γ in Fig. 1(b), passes through zero at $\gamma = 0$, shows an inflexion point at $\gamma = 1/3$, reaches a maximum at $\gamma = 2/3$ and falls to zero at $\gamma = 1$. The rate of removal is again a straight line, its gradient the inverse of (Da).

For slow flowrates there are three intersections hence three stationary-state solutions. One of these is at $\gamma_1 = 0$, one in the range $0 < \gamma_2 < (1/2)$, the third in the range $(1/2) < \gamma_3 < 1$. As the flowrate increases, the two non-zero intersections move closer together; they merge at $\gamma_2 = (1/2)$ and the loss line becomes tangential to the production curve when $(Da) = 16/27$. For yet higher flow-rates the non-zero solutions disappear, and the reaction is extinguished.

The condition for multistability is, therefore

$$(Da) > \frac{16}{27} \quad \text{or} \quad \frac{1}{4} t_{res} > 1/k a_0^2.$$

The non-zero intersections are given by the roots of a quadratic equation

$$\gamma_{2,3} = \frac{1}{2}\left\{1 \pm \sqrt{\left(1 - \frac{16}{27}(Da)^{-1}\right)}\right\}; \ \gamma_1 = 0.$$

Stability of stationary-states

If a stationary-state is perturbed by a small amount $\Delta\gamma_0$, then variation of this displacement $\Delta\gamma$ in time will be given by

$$\frac{d\Delta\gamma}{d\tau} = \lambda\Delta\gamma + \mu(\Delta\gamma)^2 + \ldots \tag{7}$$

where the partial-differential coefficients

$$\lambda = \frac{\partial}{\partial\gamma}\left(\frac{d\gamma}{d\tau}\right) \quad \text{and} \quad \mu = \frac{1}{2}\frac{\partial^2}{\partial\gamma^2}\left(\frac{d\gamma}{d\tau}\right)$$

are evaluated at the stationary-state. For *small* perturbations, such that

$$|\mu(\Delta\gamma_0)^2| \ll |\lambda\Delta\gamma_0| \tag{8}$$

the displacement at any time τ is given by

$$\Delta\gamma(\tau) = \gamma - \gamma_{ss} = \Delta\gamma_0 \exp(-\tau/\tau_*) \tag{9}$$

where $\tau_* = -1/\lambda$. Thus if λ *is negative*, the stationary-state will be *stable*, because small perturbations will decay exponentially. If λ *is positive* the perturbation will grow in time and the solution is, therefore, *unstable*. For the special case $\lambda = 0$, which occurs when the production and loss lines intersect tangentially, τ_* is apparently infinite, but here a further analysis is required as condition (8) can no longer be satisfied. This point will be discussed later.

For the *simple, quadratic* autocatalysis we find from eqn (4)

$$\lambda_1 = 4 - (Da)^{-1} \quad \text{at} \quad \gamma_1 = 0$$
$$\lambda_2 = (Da)^{-1} - 4 \quad \text{at} \quad \gamma_2.$$

Clearly λ_1 and λ_2 must have opposite signs and hence γ_1

and γ_2 have opposite stability. When γ_2 is positive it is stable, because λ_2 is negative; γ_1 will then be unstable. If (Da) is less than 1/4, so that only γ_1 is physically realistic, λ_1 is positive so the origin is stable.

For the *cubic* autocatalysis, from eqn (6)

$$\lambda_1 = -(Da)^{-1} \quad \text{at} \quad \gamma_1$$

$$\lambda_2 = \frac{27}{4}\gamma_2(1-2\gamma_2) \quad \text{at} \quad \gamma_2$$

$$\lambda_3 = \frac{27}{4}\gamma_3(1-2\gamma_3) \quad \text{at} \quad \gamma_3.$$

Thus γ_1, occurring at the origin, is stable for all flowrates because λ_1 is always negative. The second solution γ_2 lies between 0 and (1/2) and is unstable; λ_2 being positive. The third intersection λ_3 is stable as λ_3 is negative. When $(Da) = 16/27$ and $\gamma_2 = \gamma_3 = (1/2)$, λ_2 and λ_3 become zero, and the exponential form of eqn (9) no longer holds.

3. PRODUCT INFLOW, CHEMICAL REVERSIBILITY AND CATALYST DECAY

Both for the simple, quadratic and for the cubic forms of autocatalysis, one of the stationary-states represents zero reactant conversion ($\gamma = 0$). There is also no means by which the reaction can get started and move to the other stationary-states. This is equivalent to finding an infinite induction period in a closed-vessel. The problem of "nucleation" can be avoided by either of two methods: including a finite concentration of B in the inflow, or by the presence of an extra, uncatalysed reaction producing B from A. We will concentrate on the first of these. The two processes are equivalent for "simple" autocatalysis, and have similar effects for cubic autocatalysis.

Simple autocatalysis: inflow contains catalyst

The dimensionless mass-balance equation can be written as

$$\frac{d\gamma}{d\tau} = 4(\gamma+\gamma_0)(1-\gamma) - \frac{1}{(Da)}\gamma \qquad (10)$$

where $\gamma_0 = b_0/a_0$, which might typically be *ca.* 10^{-6}. The rate of production(Fig. 2a) is positive and non-zero when $\gamma = 0$, rises to a maximum at $\gamma = (1/2)(1-\gamma_0)$ and falls to zero at complete conversion $\gamma = 1$. Hence the maximum is shifted from $\gamma = (1/2)$ by an amount $(1/2)\gamma_0$.

The main effect, however, is near to the origin. There is no longer a solution at $\gamma = 0$, and there is one, and only one, intersection over the range $0 \leqq \gamma \leqq 1$, for any positive flowrate. This unique stationary-state solution is stable, the corresponding λ being negative.

The variations of the stationary-state extent of conversion with the residence time (Da) for the cases $\gamma_0 = 0$ and $\gamma_0 > 0$ are shown in Fig. 3(a) and (b) respectively. The phenomena of multiplicity and extinction disappear in the second case.

Cubic autocatalysis: inflow contains catalyst

Equation (6) now becomes

$$\frac{d\gamma}{d\tau} = \frac{27}{4}(1-\gamma)(\gamma+\gamma_0)^2 - \frac{1}{(Da)}\gamma \qquad (11)$$

Again $\gamma = 0$ is not a solution of the stationary-state condition $d\gamma/d\tau = 0$. The inflexion in the production curve now occurs at $\gamma = (1/3) - (2/3)\gamma_0$, the maximum at $\gamma = (2/3) - (1/3)\gamma_0$. There may now be two loss lines which are tangential to the production curve and there will be either one or three intersections in the positive quadrant, as shown in Figure 2(b). Tangency occurs at

$$\gamma_\pm = \frac{1}{4}\{1 \pm \sqrt{(1-8\gamma_0)}\}.$$

The lower of these corresponds to the point of *ignition*, occurring when $\gamma \ll 1$ at

$$\gamma_{ign} \cong \gamma_0.$$

The upper root, corresponding to *extinction* as before, occurs at

$$\gamma_{ext} \cong \frac{1}{2} - \gamma_0.$$

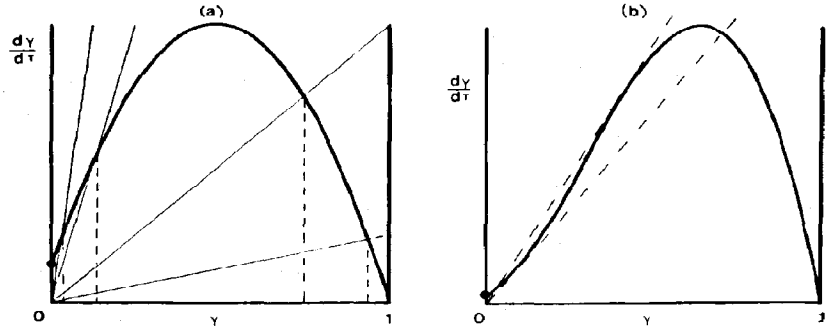

Fig. 2.

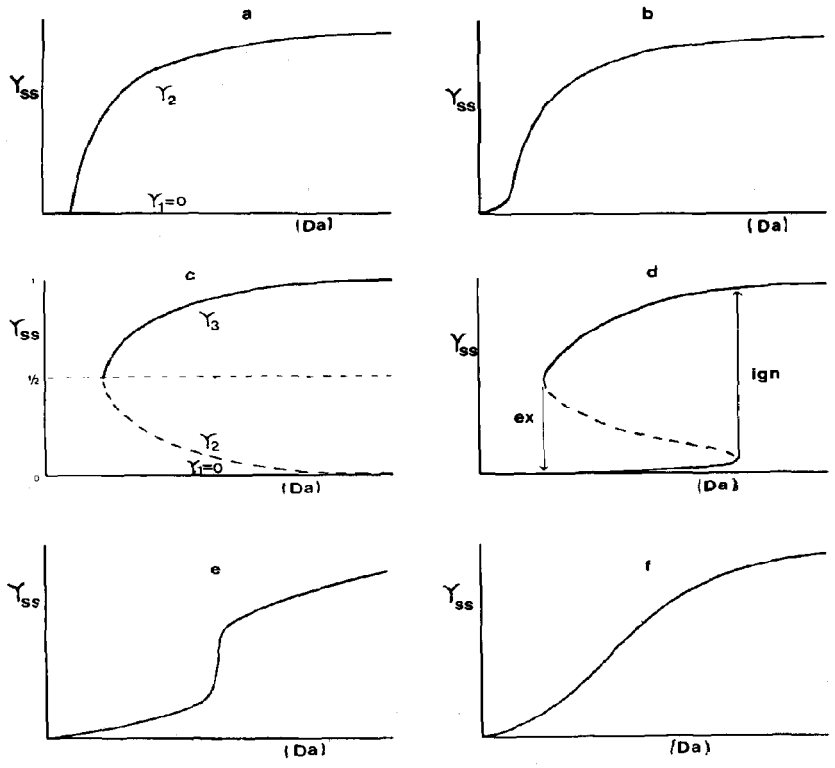

Fig. 3.

As the concentration of the autocatalytic species in the inflow increases, and γ_0 tends to (1/8) ($b_0 \rightarrow a_0/8$) so the ignition and extinction points merge and multistability disappears

For *small* values of γ_0, the range of residence times over which multistability occurs is given by

$$\frac{16}{27(1+4\gamma_0)} \leqq (Da) \leqq \frac{1}{27\gamma_0(1-2\gamma_0)}; \quad \gamma_0 \ll 1/8.$$

The variation of γ_{ss} with the Damköhler number for a number of values for γ_0 is given in Fig. 3(c)–(f).

Hysteresis. In the region of multistability the stationary-state solution of a system is dependent not only on the Damköhler number, but also on the previous history of the reactor. A system which initially has long residence-times, such that γ_3 is the only solution, will remain on this upper branch even if (Da) is reduced beyond its value at the ignition point. If the residence-time is made so short that extinction occurs, a subsequent increase in residence time will leave the system on the lower branch γ_1. Thus the region of multistability now has a region of hysteresis associated with it.

Effect of reversibility

The major effect of reversibility is to restrict the range of extent of conversion open to the system. The dimensionless mass-balance equation becomes

$$\frac{d\gamma}{d\tau} = \frac{27}{4}\gamma^2[1-(1+K_e^{-1})\gamma] - \frac{1}{(Da)}\gamma.$$

Again the first term on the r.h.s. represents the net rate of chemical production of B and is plotted as a function of γ in Fig. 4. The production curve falls to zero at γ_e, given by

$$\gamma_e = 1/(1+K_e^{-1}) = K_e/(1+K_e)$$

where $K_e = k_1/k_{-1}$ in the ratio of the forward and backward rate constants; γ_e is less than unity and represents the equilibrium extent of conversion in a closed system.

In dimensional terms, the maximum chemical production rate is reduced from its irreversible value by the factor $(1+K_c^{-1})^{-n}$. The range of residence times over which multistability occurs is reduced, but multistability does not disappear.

Reversibility, therefore, squeezes the production curve, affecting the r.h.s. of the flow-diagram (Fig. 4) qualitatively, but changing the overall behaviour only quantitatively.

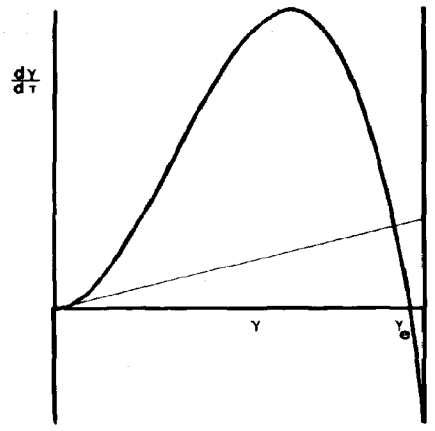

Fig. 4.

Effect of catalyst decay

When the catalyst B is absolutely stable but undergoes decay, there is a restriction on the maximum degree of conversion possible and the maximum reaction rate is affected. Superficially these consequences may seem like those of introducing the reverse reaction, but they give rise in fact to profound differences. We explore these in the remainder of the paper.

4. "EXOTIC" BEHAVIOUR: ISOLAS AND MUSHROOMS IN PATTERNS OF STATIONARY STATES

All the foregoing has concerned isothermal autocatalysis with a perfectly stable catalytic product. In real systems, catalysts may not last forever unchanged. The simplest representation of catalyst decay is:

$$B \rightarrow \text{products}; \quad \text{rate} \propto [B].$$

When this possibly is included, we find phenomena previously associated either with self-heating and heat losses or with very complex isothermal kinetics. These include isolas—closed curves in the conversion vs residence-time plane—mushrooms and sustained oscillations. It is our purpose to illustrate this here. They cannot occur in the simple, single reaction scheme (Section 3 above), but require two independent variables. Hence we must decouple the concentrations of A and B, which hitherto have been linked by the reaction stoichiometry to the inlet concentrations, eqn (3). This decoupling arises automatically if the autocatalytic product species B is not absolutely stable, but undergoes decay, either homogeneously or heterogeneously.

Thus we consider the two reaction scheme

$$A + nB \rightarrow (n+1)B \quad \text{rate} = k_1 ab^n$$
$$B \rightarrow \text{inert} \quad \text{rate} = k_2 b$$

with $n = 1$ or 2. Analogies between this and the irreversible, first-order exothermic reaction in a non-adiabatic system will be mentioned later. In the latter case the concentration of the autocatalytic species is replaced by the degree of self-heating, and the additional catalyst-decay step corresponds to Newtonian heat-loss at and through the vessel walls.

Although isolas, mushrooms and sustained oscillations occur only for cubic autocatalysis ($n = 2$), the simpler, quadratic form ($n = 1$) shows more varied behaviour than it previously did.

The time-dependent nature and stability of the various stationary-states is considered in the next section. We first turn to the dependence of the stationary-state extent of conversion on the residence-time.

Because the species B is no longer indefinitely stable the simple relationship embodied in eqn (3), $a_0 = a + b$ no longer holds, and thus the two possible choices for the dimensionless measure of extent of reaction

$$\gamma = \frac{a_0 - a}{a_0} \quad \text{and} \quad \gamma = \frac{b}{a_0}$$

are no longer equivalent, nor even simply related. For convenience we choose the former of these definitions, in terms of a_0 and a. (In a more extended treatment we should need to introduce separate variables $\alpha = a/a_0$ and $\beta = b/b_0$.)

Simple, quadratic autocatalysis with decay

The two mass-balance equations are

$$-\frac{da}{dt} = k_1 ab - k_{res}(a_0 - a) \tag{12i}$$

and

$$\frac{db}{dt} = k_1 ab + k_{res}(b_0 - b) - k_2 b. \tag{12ii}$$

In the *stationary-state*, both time-derivatives are zero and we have the extra condition from combining (12i) and (12ii)

$$b_{ss} = \left(\frac{k_{res}}{k_2 + k_{res}}\right)(a_0 + b_0 - a_{ss}). \tag{13}$$

This equation applies *only* at the stationary-state but clearly reduces to the restriction of (3) as k_2 tends to zero.

If we first assume $b_0 = 0$, and substitute (13) into (12i) we obtain

$$\gamma_{ss}(1 - \gamma_{ss}) - \frac{\gamma_{ss}}{\tau_{res}}\left(\frac{\tau_{res}}{\tau_2} + 1\right) = 0. \tag{14}$$

Here τ_{res} and τ_2 are dimensionless residence-time† and reaction-time for step 2, respectively:

$$\tau_{res} = k_1 a_0 t_{res}$$

$$\tau_2 = k_1 a_0 t_2 = k_1 a_0 / k_2.$$

†Note that the characteristic chemical time-scale used here will be $1/k_1 a_0^n$, rather than that based on the maximum rate used earlier—see Discussion.

One solution of (14) is $\gamma_{ss} = \gamma_1 = 0$, as found in section 2; for the non-zero stationary-state we may divide each term by γ_{ss}. The resulting equality is:

$$(1 - \gamma_2) = \frac{1}{\tau_{res}}\left(\frac{\tau_{res}}{\tau_2} + 1\right)$$

or

$$\gamma_2 = 1 - \frac{1}{\tau_{res}} - \frac{1}{\tau_2}. \qquad (15)$$

Clearly γ_2, the second intersection, cannot reach the value unity (complete conversion of A) even if the residence time becomes infinite, because $1/\tau_2$ is not zero. There is also a lower limit on τ_{res} for γ_2 to remain positive, depending on τ_2. The value of γ_2 increases monotonically as τ_{res} increases.

Figure 5(a) shows the flow diagram corresponding to (14); the loss-line has a gradient of $(1/\tau_{res}) + (1/\tau_2)$, which tends to $1/\tau_2$ as τ_{res} tends to infinite values. Hence, if τ_2 is less than unity ($k_2 > k_1 a_0$), γ_2 cannot be positive. The dependence of the extent of conversion on the residence-time is given in Fig. 5(b) for $\tau_2 > 1$.

Again, a non-zero inflow of b ($\gamma_0 > 0$) removes multiplicity; instead, a unique solution γ_1 exists for all τ_{res} and τ_2. This is shown in Fig. 5(c) and (d).

Apart from limiting the range available for γ_2, the decay of the catalyst has introduced no new patterns to the γ_{ss}–τ_{res} curve. Some important differences do arise, however, concerning the stability of the upper solution γ_2; these will be developed in the next section (Section 5). Extinction still occurs, and can be caused either by fast flow, or by a fast rate of catalyst decay.

Cubic autocatalysis with decay

For cubic autocatalysis we now have

$$-\frac{da}{dt} = k_1 ab^2 - k_{res}(a_o - a) \qquad (16i)$$

$$\frac{db}{dt} = k_1 ab^2 + k_{res}(b_0 - b) - k_2 b \qquad (16ii)$$

The stationary-state relationship (13) between a_{ss} and b_{ss} still holds (it is valid for all n). We will treat the algebraically simpler case $b_0 = 0$ first, and then generalize to allow for the inflow of B.

Inflow is pure A

From (13) and (16), the relationship between γ_{ss} and the residence time τ_{res} is given by

$$\gamma_{ss}^2(1 - \gamma_{ss}) - \frac{1}{\tau_{res}}\left(\frac{\tau_{res}}{\tau_2} + 1\right)^2 \gamma_{ss} = 0 \qquad (17)$$

where

$$\tau_{res} = k_1 a_0^2 t_{res};\ \tau_2 = k_1 a_0^2/k_2.$$

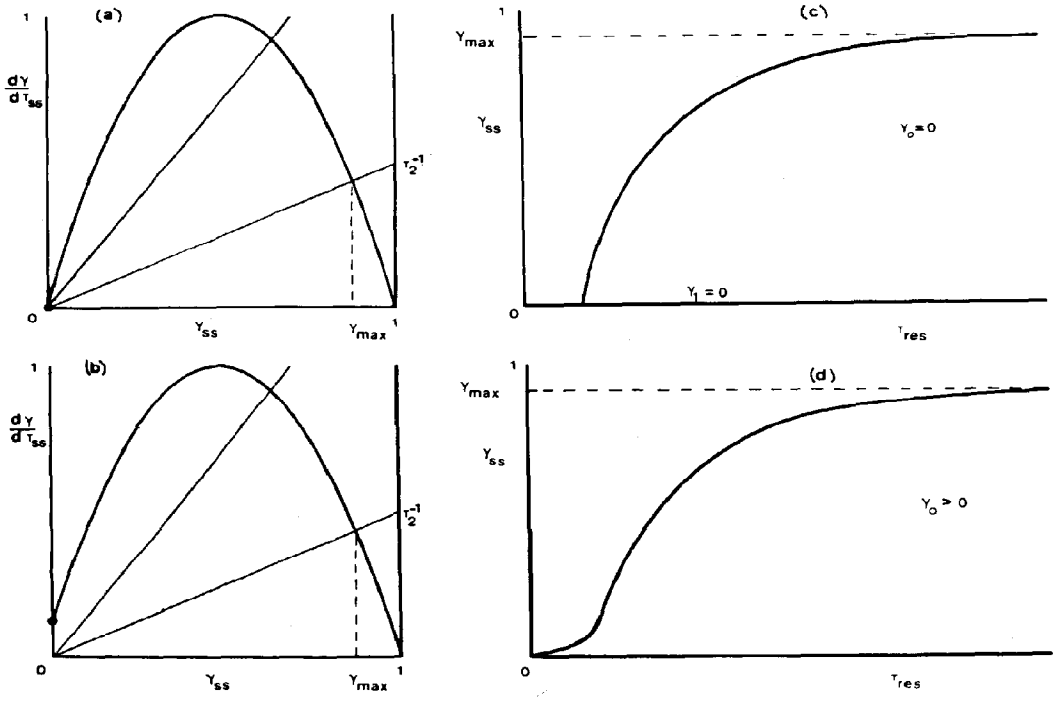

Fig. 5.

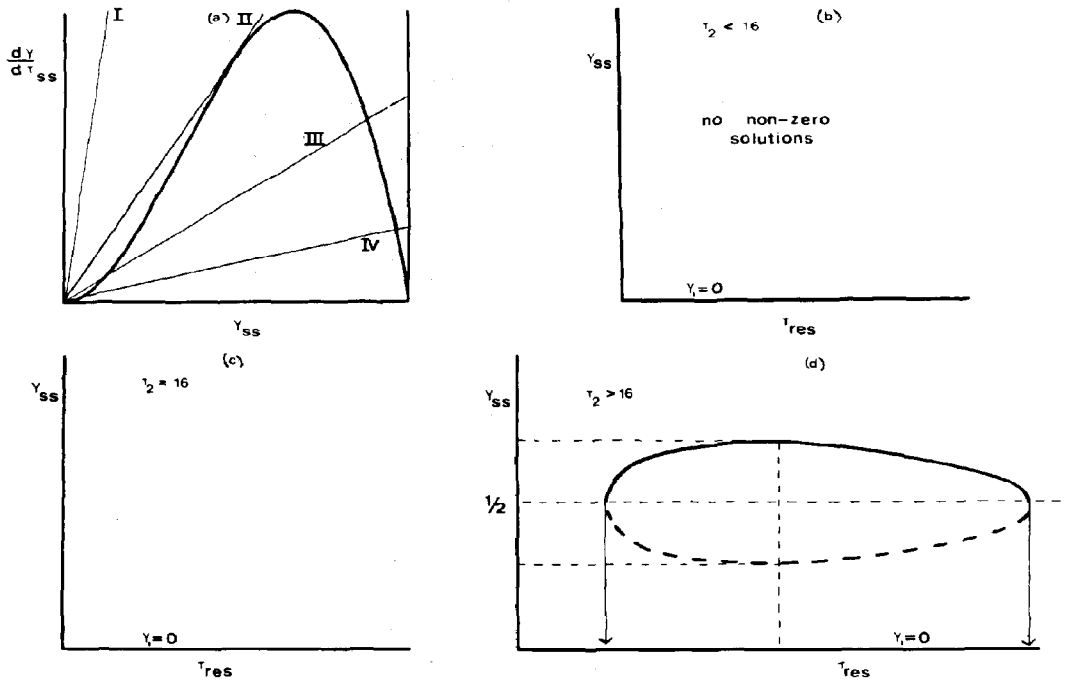

Fig. 6.

Equation (17) is analogous to (14), with a higher power of γ_{ss} in the first term, which represents the chemical production rate in the stationary-state. The second term, the overall rate of removal, is also of higher degree, being quadratic in τ_{res}.

One stationary-state solution is $\gamma_1 = 0$, the other two are given by the roots of

$$\gamma_{ss}(1-\gamma_{ss}) = \frac{1}{\tau_{res}}\left(\frac{\tau_{res}}{\tau_2}+1\right)^2. \qquad (18)$$

Over some range of conditions (18) may yield *two* possible residence-times for a given γ_{ss} and *two* stationary-state conversions γ_2 and γ_3 for a given value of τ_{res}. The multiplicity of solutions of τ_{res} is a new feature, not occurring when the catalyst is stable ($k_2 = 0$).

The condition that this multiplicity exists over some range of γ_{ss} and τ_{res} is

$$\frac{1}{4} > \frac{4}{\tau_2}, \quad \text{i.e.} \quad k_2 < \frac{1}{16}k_1 a_0^2 \qquad (19)$$

This arises because the maximum of the l.h.s. of (18) is 1/4 and the minimum of the r.h.s. as τ_{res} varies is $4/\tau_2$.

When inequality (19) is satisfied, the second and third stationary-states lie on an isolated, closed curve or isola (see Fig. 6d).

The existence of the isola, and its size may be explained by reference to the flow diagram corresponding to (17). The production curve has the familiar cubic form, and the loss-line is linear in γ with a gradient related to τ_{res}. Very short residence times give rise to a very steep gradient. Lengthening the residence time reduces the steepness, but the gradient cannot decrease to zero, as it did in the absence of product decay. Instead, it has a minimum value of $4/\tau$ when $\tau_{res} = \tau_2$. The position of this line of minimum slope relative to the tangent line, which has a gradient of 1/4 determines the number of intersections possible, and hence the pattern of the dependence of γ_{ss} on τ_{res}. The variety of possibilities is displayed in Figs. 6(a)–(d).

The flow diagram for eqn (17) is shown in Fig. 6(a). When inequality (19) is *not* satisfied the loss-line of minimum slope is represented by line (I). The gradient of this line exceeds 1/4 and the only intersection with the production curve is at the origin, $\gamma_1 = 0$. Thus the stationary-state solution is unique and zero for all residence times (Fig. 6b). If (19) becomes an equality, the loss-line of minimum slope, which corresponds to $\tau_{res} = \tau_2$, is the same as the tangent to the production curve. This is shown by line II in Fig 6(a), with the dependence of γ_{ss} on τ_{res} shown in 6(c). Again $\gamma_1 = 0$ is a solution for all τ_{res}, but there is a second solution, $\gamma_2 = (1/2)$ at $\tau_{res} = \tau_2$. This represents the onset of multistability and the "birth" of the isola.

When (19) is satisfied, the loss-lime of minimum slope lies below the tangent line and is represented by line IV. For the shortest residence times, the loss line is steep

and only intersects the production curve at the origin. Increasing the residence time decreases the slope of the loss line and when it has a gradient equal to that of the tangent (curve II, Fig. 6(c)) a second intersection occurs $\gamma_2 = \gamma_3 = (1/2)$. Further increase of the residence time causes the loss-line to become yet flatter (curve III, Fig. 6(a) and there will be three intersections. When $\tau_{res} = \tau_2$ the loss-line reaches its minimum slope (curve IV) and further increases in the residence time results in the above sequence to be re-traced in reverse. The second and third intersections come closer together again and merge at the tangency, $\gamma_2 = \gamma_3 = (1/2)$. Thus the resulting isola, shown in Fig. 6(d), is symmetrical about $\gamma_{ss} = (1/2)$, and it covers the widest range of γ_{ss} when $\tau_{res} = \tau_2$.

The isola extends over a range of residence-times $\tau_{res}^{-} \leqq \tau_{res} \leqq \tau_{res}^{+}$, where $\tau_{res}^{\pm}$ represent the residence-times for which the slope of the loss line is equal to the tangent slope, i.e. for which

$$\frac{1}{\tau_{res}}\left(\frac{\tau_{res}}{\tau_2}+1\right)^2 = \frac{1}{4}$$

or

$$\tau_{res}^{\pm} = \tau_2\left\{\frac{1}{8}\tau_2 - 1 \pm \sqrt{\left[\tau_2\left(\frac{\tau_2}{16}-1\right)\right]}\right\}.$$

Inflow contains B

If we include the autocatalytic species B in the inflow, and denote $\gamma_0 = b_0/a_0$, the stationary-state relationship becomes

$$(\gamma_{ss} + \gamma_0)^2)1 - \gamma_{ss}) = \frac{1}{\tau_{res}}\left(\frac{\tau_{res}}{\tau_2}+1\right)^2 \gamma_{ss} \qquad (20)$$

The range of flow-diagrams and the accompanying dependence of γ_{ss} on τ_{res} corresponding to (20) are shown in Fig. 7 (a)–(f), for a "small" value of γ_0 (i.e. $\gamma_0 < (1/8)$).

The production curve has two tangencies, occurring for *small* γ_0 at degrees of conversion given approximately by

$$\gamma_{ss} = \gamma_0 \quad \text{and} \quad \frac{1}{2} - \gamma_0$$

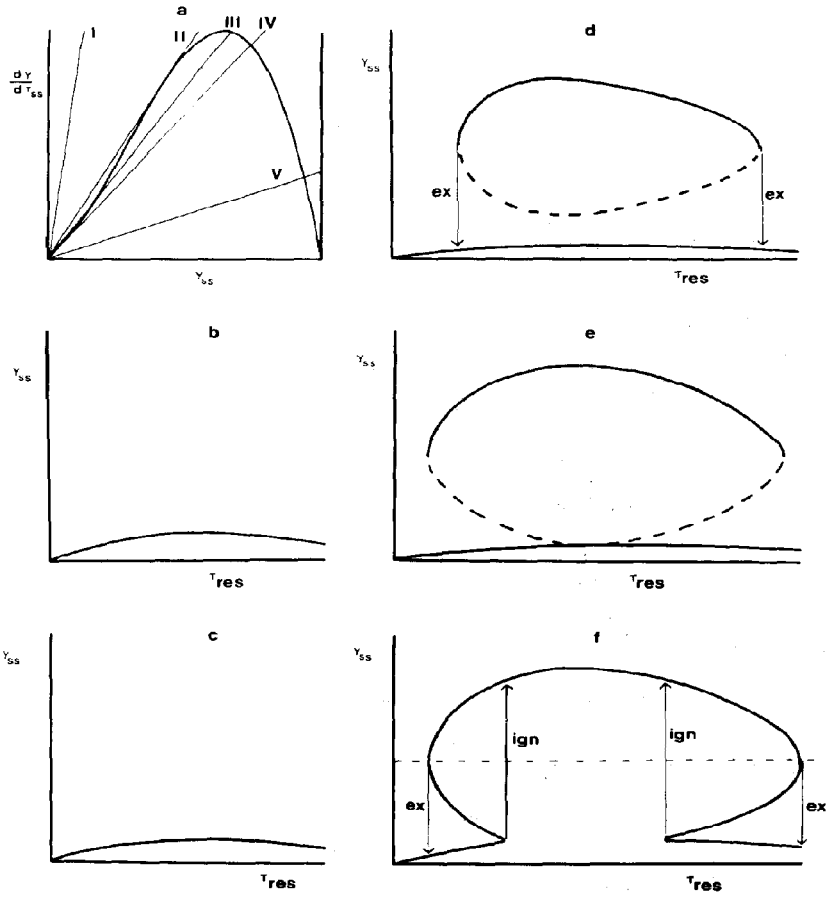

Fig. 7.

with slopes of $4\gamma_0(1-2\gamma_0)$ and $((1/4)+\gamma_0)$ respectively. It is the relative positions of these two tangents and the loss-line of minimum slope that dictates the nature of the $\gamma_{ss}-\tau_{res}$ diagram. The minimum slope of the removal line again is $4/\tau_2$, occuring at $\tau_{res}=\tau_2$.

If the minimum slope exceeds the upper tangent, then only a unique intersection γ_1, close to the origin exists. This is shown in Fig. 7(b). The onset of an isola (Fig. 7c) again occurs when the loss-line has a minimum slope equal to the upper tangent, line II in Fig. 7(a).

If the loss-line of minimum slope lies between the two tangent curves, i.e. if

$$4\gamma_0(1-2\gamma_0)<4/\tau_2<\frac{1}{4}+\gamma_0 \tag{21}$$

the $\gamma_{ss}-\tau_{res}$ dependence shows isola behaviour, Fig. 7(d). An isola has two extinction points, corresponding to the loss line crossing the upper tangent as τ_{res} is varied; there are no ignition points, because the lower tangent is not reached. In addition to solutions on the isola, the lower branch on Fig. 7(d), corresponding to γ_1 is non-zero.

Extra forms of behaviour are now possible. If the minimum loss-line coincides with the lower tangent (curve IV), the isola and the lower branch just touch as shown in Fig. 7(e). In some cases the loss-line may lie below the lower tangent. The condition for this is

$$4/\tau_2<4\gamma_0\,(1-2\gamma_0). \tag{22}$$

The variation of γ_{ss} with τ_{res} in this situation is shown in Fig. 7(f). The isola has now merged with the lower branch to give a "mushroom". There are now two ignition points as well as the extinctions, and two regions of hysteresis over which multistability occurs. In between these regions there is a range of residence-times for which a unique solution exists, corresponding to the γ branch.

The upper range of γ_{ss} is now accessible to the system (it existed but could not be attained for the isolas). Once the residence time and inlet concentration of B have been manipulated in order to obtain a stationary-state extent of conversion at the top of the mushroom, corresponding to curve (V) in Fig. 7(e) and (f), a reduction in γ_0 will cause the mushroom to change to an isola. In this way the upper range of the isola, which represents stable solutions, can be reached.

As k_2 tends to zero ($\tau_2\to\infty$), the range of residence-times covered by the mushroom becomes infinite, and the S-shape dependence of γ_{ss} on τ_{res} found for the stable product in the previous section is recovered.

For large inflow concentrations of B, $\gamma_0\geqq(1/8)$, the tangents to the production curve merge and then disappear. Only unique solutions are now found, with their maximum stationary-state conversions occurring when $\tau_{res}=\tau_2$.

For the cubic autocatalysis, therefore, there is a dramatic change in the behaviour observer, if the catalyst is allowed to become in the least bit unstable. This instability may be the result either of further chemical reaction (homogeneous or heterogeneous) or due to poisoning or to some physical degradation.

5. STABILITY OF STATIONARY-STATES: OSCILLATORY SOLUTIONS

The final point that we shall investigate is the effect of the decay reaction on the pattern of stability encountered. A full investigation will be reported elsewhere but here we illustrate some of the variety of behaviour possible, with particular reference to mushrooms. Because the concentrations a and b are now decoupled, the various algebraic relationships derived above holding *only in the stationary-state*, a new dimension is added to the range of behaviour possible. Again we shall investigate the response of the various stationary-state solutions to small perturbations: where "small" is used in the sense of earlier, allowing us to neglect all but linear powers of the perturbation. The initial time-dependence of the perturbations can then be expressed as

$$\Delta a=\alpha_1\exp(\lambda_1 t)+\alpha_2\exp(\lambda_2 t)$$

$$\Delta b=\beta_1\exp(\lambda_1 t)+\beta_2\exp(\lambda_2 t).$$

The detailed behaviour is thus expressed by the sign and nature of the exponents λ_1 and λ_2, which are given by the roots of the characteristic equation:

$$\begin{vmatrix} \frac{\partial}{\partial a}\left(\frac{da}{dt}\right)-\lambda & \frac{\partial}{\partial b}\left(\frac{da}{dt}\right) \\ \frac{\partial}{\partial a}\left(\frac{db}{dt}\right) & \frac{\partial}{\partial b}\left(\frac{db}{dt}\right)-\lambda \end{vmatrix}=0$$

The roots of this quadratic may be positive or negative, real or complex, and these determine the pattern of responses observed.

We shall find that for the simple autocatalysis, the zero intersection γ_1 is unstable when the non-zero solution γ_2 is positive and stable. With cubic autocatalysis the stability of the first two intersections γ_1 (stable) and γ_2 (unstable) is unchanged, but the highest stationary-state γ_3 is not always stable.

Simple, quadratic autocatalysis

For suitable values of τ_{res} and τ_2 this system has two realizable stationary-states (see Section 4), $\gamma_1=0$ and $\gamma_2>0$. When this is so the lower solution γ_1 is unstable. It is a saddle point; after the smallest departure it is never revisited. The upper solution γ_2 is always stable, but two different stable solutions are possible: one is accompanied by a monotonic decay of a and b to the stationary-state (stable node); the other returns via a series of damped oscillations (stable focus). Thr range of focal behaviour separates two ranges of nodal behaviour on the γ_{ss} axis and is given by

$$\frac{1}{\tau_{res}}\left(1+\frac{\tau_{res}}{\tau_2}\right)^2\left[1-\left(\frac{\tau_{res}}{\tau_2+\tau_{res}}\right)^{1/2}\right]^2\leqq\gamma_{ss}$$

$$\leqq\frac{1}{\tau_{res}}\left(1+\frac{\tau_{res}}{\tau_2}\right)^2\left[1+\left(\frac{\tau_{res}}{\tau_2+\tau_{res}}\right)^{1/2}\right]^2. \tag{23}$$

The different regions are indicated in Fig. 8(a) for $\tau_2=20$. This diagram is, however, only a two-dimen-

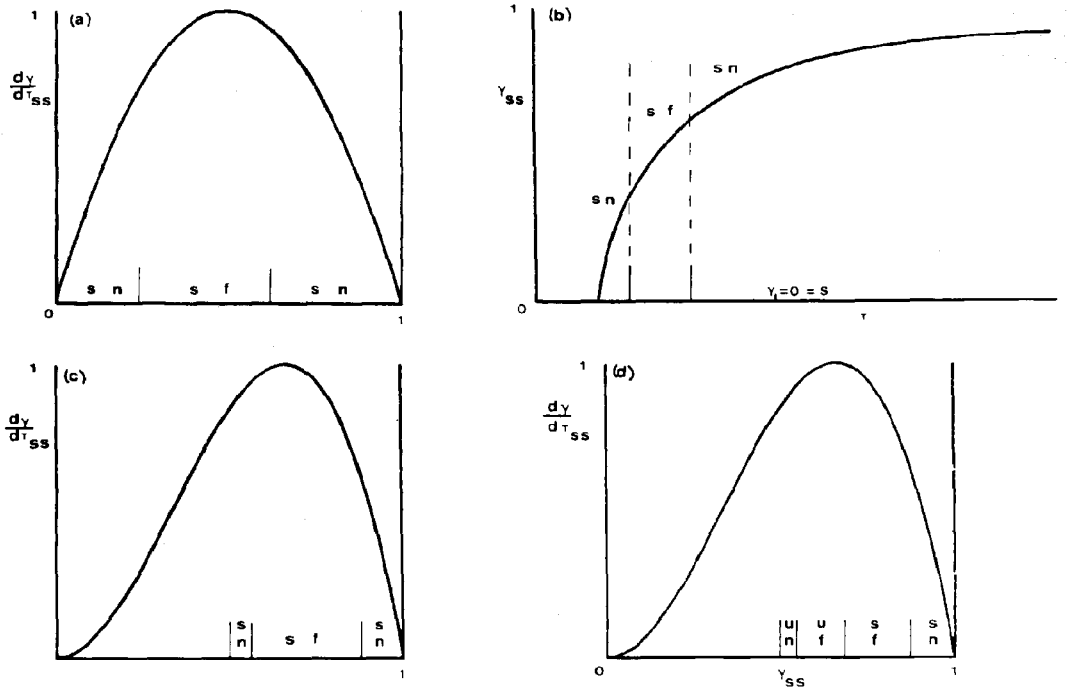

Fig. 8.

sional representation of a three-dimensional system; the division of the γ_{ss}-axis into different regions is such that each range (stable node, stable focus) indicates the nature of any intersection of the gain and loss lines which might occur directly above it. The limits of the range in (23) themselves vary with γ_{res}, as does the solution γ_2, and they therefore represent a moving range or "window" of focal behaviour, which slides along the γ_{ss} axis. The upper limit is not monotonic with τ_{res}. At first it decreases as the residence-time is increased, but after passing through a minimum it increases again. Hence a region of focal behaviour can exist at long residence times as shown in Fig. 8(b). As τ_{res} tends to infinite values, however, nodal behaviour must return.

Cubic autocatalysis: $\gamma_0 = 0$

The condition for there to be three stationary-states has been given in terms of τ_{res} and τ_2, in Section 4, eqn (19). When this is satisfied the origin γ_1 is always found to be stable. The second solution γ_2 is always unstable, a saddle point. Again, the decoupling of a and b introduces a wider range of behaviour open to the highest stationary-state γ_3.

There are two situations, which lead to different patterns: first if the rate constant k_2 is less than that for flow $k_{res} = 1/t_{res}$ (i.e. if $\tau_{res} < \tau_2$); in the second case k_2 exceeds k_{res}, or the residence time is longer than the characteristic reaction time for the decay reaction ($\tau_{res} > \tau_2$).

In the first case ($k_2 \leqq k_{res}$; $\tau_{res} < \tau_2$) the third intersection γ_3 is always stable, but may show either nodal or focal behaviour. The ranges of γ_3 over which these different characters occur are given in Table 1. This system cannot show sustained, undamped oscillations (limit cycles). The division of the γ_{ss} axis into the five ranges possible (node-saddle-node-focus-node) is shown in Fig. 8(c).

This behaviour describes the system over the range of residence times for which the gradient of the loss-line is decreasing as τ_{res} is increased (the minimum slope occurs when $\tau_{res} = \tau_2$). Beyond this the relative magnitudes of k_2 and k_{res} are reversed ($k_2 > k_{res}$; $\tau_2 < \tau_{res}$), and there are *four* possible types of behaviour open to γ_3. These are illustrated in Fig. 8(d). Immediately to the right of $\gamma_{ss} = (1/2)$ (the lower limit on γ_3) is a region of unstable nodes. Here γ_1 and γ_2 are real and both are positive. Higher values of γ_{ss} correspond to unstable local behaviour (λ_1 and λ_2 complex with positive real parts). Unstable foci may be surrounded by stable limit-cycles, corresponding to sustained, stable oscillations. As γ_3 takes higher values the foci become stable and finally damped oscillations give way to monotonic responses, and stable, nodal character. The ranges of γ_3, in terms of τ_2 and τ_{res}, over which these different patterns occur are given in Table 2.

When γ_0 is not equal to zero one can obtain mushrooms as well as isolas. The lowest solution γ_1 is not zero. The equations determining the character of the

Table 1. Character of the different stationary-states for cubic autocatalysis with catalyst decay, $k_2 \leqq k_{res}$, $\tau_{res} \leqq \tau_2$

Stationary-state	range	character
1	$\gamma_1 = 0$	stable node
2	$0 < \gamma_2 < \frac{1}{2}$	saddle point
3	$\frac{1}{2} < \gamma_3 < (1+\frac{\tau_{res}}{\tau_2})\{[2(\frac{1}{\tau_2}+\frac{1}{\tau_{res}})]^{\frac{1}{2}} - (\frac{1}{\tau_2})^{\frac{1}{2}}\}$	stable node
	$(1+\frac{\tau_{res}}{\tau_2})\{[2(\frac{1}{\tau_2}+\frac{1}{\tau_{res}})]^{\frac{1}{2}} - (\frac{1}{\tau_2})^{\frac{1}{2}}\} < \gamma_3 < (1+\frac{\tau_{res}}{\tau_2})\{[2(\frac{1}{\tau_2}+\frac{1}{\tau_{res}})]^{\frac{1}{2}} + (\frac{1}{\tau_2})^{\frac{1}{2}}\}$	stable focus
	$(1+\frac{\tau_{res}}{\tau_2})\{[2(\frac{1}{\tau_2}+\frac{1}{\tau_{res}})]^{\frac{1}{2}} + (\frac{1}{\tau_2})^{\frac{1}{2}}\} < \gamma_3 < 1$	stable node

Table 2. Character of the different stationary-states for cubic autocatalysis with catalyst decay; $k_2 > k_{res}$, $\tau_2 < \tau_{res}$

Stationary-state	range	character
1	$\gamma_1 = 0$	stable node
2	$0 < \gamma_2 < \frac{1}{2}$	saddle point
3	$\frac{1}{2} < \gamma_3 < (1+\frac{\tau_{res}}{\tau_2})\{[2(\frac{1}{\tau_2}+\frac{1}{\tau_{res}})]^{\frac{1}{2}} - (\frac{1}{\tau_2})^{\frac{1}{2}}\}$	unstable node
	$(1+\frac{\tau_{res}}{\tau_2})\{[2(\frac{1}{\tau_2}+\frac{1}{\tau_{res}})]^{\frac{1}{2}} - (\frac{1}{\tau_2})^{\frac{1}{2}}\} < \gamma_3 < (1+\frac{\tau_{res}}{\tau_2})(\frac{1}{\tau_2})^{\frac{1}{2}}$	unstable focus
	$(1+\frac{\tau_{res}}{\tau_2})(\frac{1}{\tau_2})^{\frac{1}{2}} < \gamma_3 < (1+\frac{\tau_{res}}{\tau_2})\{[2(\frac{1}{\tau_2}+\frac{1}{\tau_{res}})]^{\frac{1}{2}} + (\frac{1}{\tau_2})^{\frac{1}{2}}\}$	stable focus
	$(1+\frac{\tau_{res}}{\tau_2})\{[2(\frac{1}{\tau_2}+\frac{1}{\tau_{res}})]^{\frac{1}{2}} + (\frac{1}{\tau_2})^{\frac{1}{2}}\} < \gamma_3 < 1$	stable node

different intersections are not so easily transformed into a series of ranges of γ_{ss}, such as those in Tables 1 and 2 for $\gamma_0 = 0$.

Stability is ensured if

$$k_1 b_{ss}^2 - k_2 + 2k_{res}\frac{b_0}{b_{ss}} > 0$$

or, in terms of γ etc.

$$\frac{(\gamma+\gamma_0)^2}{(1+\kappa)^2} + 2\gamma_0\frac{(1+\kappa)}{(\gamma+\gamma_0)} > \frac{1}{\tau_2}$$

where $\kappa = \tau_{res}/\tau_2$. For $b_0 = a_0\gamma_0 = 0$ this reduces to a simple quadratic form.

The condition distinguishing between nodal and focal states (real and complex λ respectively) is similarly more complicated: for $\gamma_0 = 0$, it is a biquadratic; for $\gamma_0 > 0$ it is of degree 6.

Figure 9 shows the dependence of γ_{ss} on τ_{res} for three different cases (different values of τ_2 and γ_0), with the stability of the solutions indicated. In Fig. 9(a) $\gamma_0 = 0$ and $\tau_2 = 20$. An isola extends over $7.64 \leqq \tau_{res} \leqq 52.4$ covering a range of γ_{ss} of $0.724 \leqq \gamma_{ss} \leqq 0.276$. The lowest solution $\gamma_1 = 0$ extends over all residence times and is a stable node. The middle solution γ_2 is always an unstable, saddle point. Four different stabilities are seen for γ_3. At the l.h.s. of the isola ($\tau_{res} < 35$) this upper solution is *stable*, and for much of this range has *focal* character. For higher residence times γ_3 at first retains its focal nature, but becomes *unstable*. Just before disappearing (merging with the saddle point γ_2) the upper solution becomes an *unstable node*. Notice that focal behaviour is much more widespread than nodal; indicating that a perturbed system is more likely to return by a series of damped over- and undershoots (ringing) than to be overdamped. Unstable foci are prime candidates for regions of stable limit cycles (sustained oscillations), but must be unique for limit cycles to occur definitely.

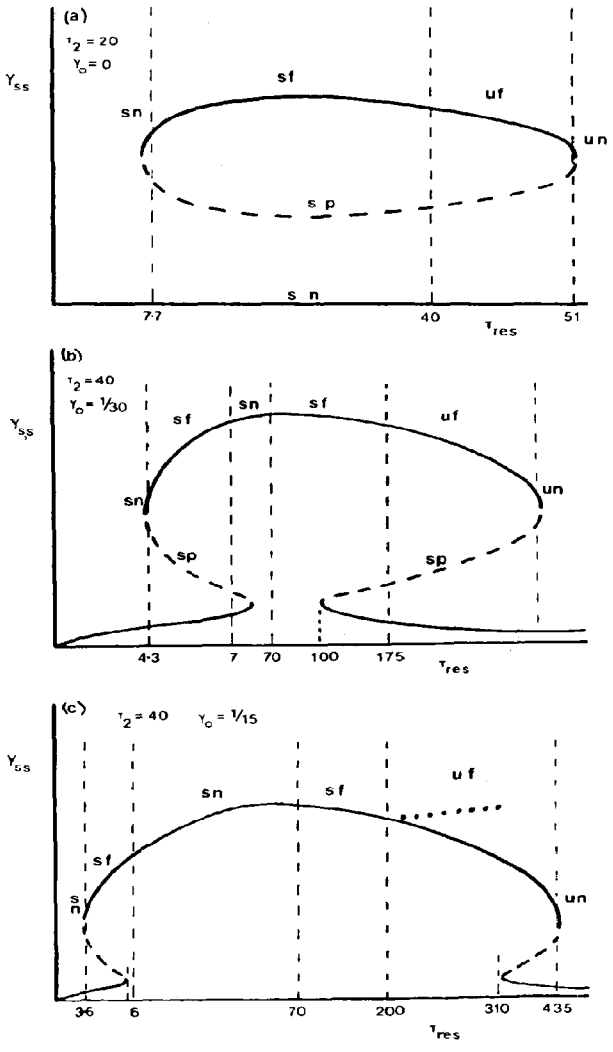

Fig. 9.

Figure 9(b) represents $\tau_2 = 40$, $\gamma_0 = 1/30$. The $\gamma_{ss} - \tau_{res}$ curve is a mushroom. The lowest intersection γ_1 lies above the τ_{res} ($\gamma_{ss} = 0$) axis, and over much of its range it has *stable focal* character. The pattern observed for γ_3 is wider than that for the isola above, but again the l.h.s. represents stable solutions. The wide range of stable focal is now interrupted by a region of stable nodes: this is a consequence mainly of increasing τ_2, and may be observed in isolas. For $\tau_{res} > 200$, γ_3 becomes an *unstable focus*, but at these residence-times γ_3 is not unique—the region of uniqueness being $10 < \tau_{res} < 111$. Thus again we cannot guarantee stable limit cycles surrounding the unstable foci (see Discussion).

In Fig. 9(c) $\gamma_0 = 1/15$ and $\tau_2 = 40$. Increasing γ_0 has extended the range of τ_{res} over which the mushrooms occurs, and has also extended the range of unique, upper solutions γ_3. The lowest intersection γ_1 is a *stable focus* over much of the diagram. The second solution γ_2 is a saddle point. The upper stationary-state again changes character a number of times as τ_{res} is increased. The lowest residence-times ($\tau_{res} < 200$) correspond to stable solutions, with two ranges of stable nodes and two of stable foci. Over $200 < \tau_{res} < 310$, γ_3 is *unique*, and an *unstable focus*. In this region, therefore, one will find *stable limit cycles*, whose amplitudes increase as τ_{res} increases. These are marked on Fig. 9(c) in the style of Uppal, Ray and Poore[3]. For $310 < \tau_{res} < 435$, γ_3 is still an unstable focus, but is no longer unique. A small region of *unstable nodal* behaviour precedes the merging of γ_4 and γ_5.

6. DISCUSSION

The two cases of autocatalysis studied here cover many of the possible types of behaviour observed in more complicated systems. In particular they cover the different forms possible for the dependence of the production or gain curve on the extent of reaction. For quadratic autocatalysis the gain curve rises steeply from zero at low γ values, whilst the cubic case shows a slow rise followed by an inflexion in the rate of production curve. Both rate-laws exhibit a maximum in the gain curve, with the production rate falling to zero on complete conversion of the substrate A (or achievement of the equilibrium composition for a reversible reaction). Such dependences are illustrated by many enzyme systems (see e.g. Ref. [9]) and also in some heterogeneous catalyses, although for the latter the solid catalyst is not usually swept out of the reactor with the fluid.

Even our simple prototypes lead to a surprisingly wide variety of forms: mushrooms, isolas and the patterns of stable and unstable nodes and foci. Explicit equations in terms of various rate constants, flow-rates and initial concentrations allow the number of stationary-state solutions and the character of each to be evaluated.

For deceleratory systems the natural basis for the chemical-time incorporated into the Damköhler number involves the initial reaction rate, but for autocatalytic reactions this is zero ($\gamma_0 = 0$) or very small (γ_0 small). Here a natural base for the chemical time is the *maximum* rate, which leads to the factors 1/4 and 4/27 for the quadratic and cubic rate-laws respectively. For non-zero inlet concentrations of the autocatalytic species ($\gamma_0 \neq 0$), we have an extra factor of $(1 + \gamma_0)^{n+1}$ in the maximum rate, hence the general form for t_{chem} for *irreversible* systems are

$$t_{\text{chem}} = \frac{a_0}{(1/4)k_1 a_0^2 (1+\gamma_0)^2} \quad \text{for quadratic}$$

$$t_{\text{chem}} = \frac{a_0}{(4/27)k_1 a_0^3 (1+\gamma_0)^3} \quad \text{for cubic}$$

For *reversible* reactions, the maximum rate of chemical production is reduced, and the chemical time contains a factor $(1 + K_c^{-1})^n$ in the numerator. This scaling ensures that the maximum, dimensionless chemical production-rate takes the value unity for all systems.

In Sections 4 and 5 of this work, where we consider steady-state behaviour, we have used a different basis, using $t_{\text{chem}} = 1/k_1 a_0$ and $t_{\text{chem}} = 1/k_1 a_0^2$ for quadratic and cubic forms respectively. We have done this here because our interest is not in finding the maximum reaction rate but in revealing other features and because in this way we achieve some compactness in our results which would otherwise contain extra factors of (1/4) or 4/27. In these two sections we have not introduced a Damköhler number. We have two loss processes—decay and outflow, characterized by τ_2 and τ_{res} respectively—and we have wished to keep these separate: in practice an experimenter is often free to change the residence-time but not the rate of catalyst decay.

Flow diagrams have been particularly useful, giving clear representations of the algebraic equations. Throughout they are of great value for all aspects of the stationary behaviour: unique versus multiple solutions; hysteresis; and jumps (ignition and extinction). Maximum rates and yields are vividly illustrated; as are the effects of reversibility and of non-zero inlet concentrations of the autocatalyst. The inclusion of B in the inflow is of more significance than might be at first thought. The effect is qualitatively the same as that of having a parallel, non-catalytic reaction $A \rightarrow B$. These two processes open chinks in the armour of the lowest stationary-state $\gamma_1 = 0$, allowing other intersections to become accessible and introducing ignition. The stationary-state condition changes from

$$\gamma^{n-1}(1-\gamma) = f(\tau_{\text{res}})$$

encountered in eqn (18) to the form in (20)

$$(\gamma + \gamma_0)^n (1-\gamma) = \gamma f(\tau_{\text{res}}),$$

where $f(\tau_{\text{res}})$ is some function of the residence-time.

The flow diagrams also come into their own when explaining the occurrence of isolas and mushrooms. The algebraic analyses, even of some of the simpler equations, are by comparison somewhat opaque, and this has encouraged some wrong ideas which are clearly exposed by the relevant diagrams. These diagrams play an analogoue rôle to the thermal diagrams in non-isothermal circumstances. In the latter, the rate of heat production and heat transfer (via flow and through the reactor walls) are plotted against the reactant temperature, with intersections again representing stationary-state solutions of heat balance.

We have mentioned the analogy between the isothermal cases studied here and the non-isothermal, first-order irreversible reaction. The difference between a completely stable catalyst ($k_2 = 0$) and one which has a finite decay rate ($k_2 > 0$) mirrors the difference between adiabatic operation and the situation where heat can be transferred through the vessel walls. In particular we note that at long residence-times, $\tau_{\text{res}} \rightarrow \infty$, the two cases $k_2 = 0$ and $k_2 = \epsilon$; $\epsilon > 0$ differ both quantitatively and qualitatively no matter how small ϵ might be. For a stable catalyst the extent of conversion γ_{ss} tends to unity at long τ_{res} (similarly for an adiabatic reactor the stationary-state temperature-excess θ tends to its adiabatic value in this limit). For even the slightest instability in the catalyst or the slightest leaking of heat from the vessels γ_{ss} tends to zero for infinite residence times, just as θ tends to zero in the non-isothermal case.

Once the finite life-time of the catalyst is recognized the problem changes from one dimension to two. When the system is described by a single parameter (Sections 2 and 3) we can indicate the stability of the stationary-states by arrows-on-a-line on the flow diagram. For the less simple, two-parameter systems this interpretation is still useful and the ranges of the different stabilities can be indicated on the flow diagram, but it must be remembered that this is now a two-dimensional representation of a three-dimensional surface and that it is solely restricted to the stationary-state behaviour.

Small values of τ_2, corresponding to an unstable catalyst, mean that the loss-line is always steep and multistability may disappear as a result. This complements the disappearance of multistability caused by varying the residence-time, which can occur for any value of τ_2 and which is known as "washout".

In these cases, "small" and "large" refer to the relative magnitude of $t_2 = 1/k_2$ with respect to our characteristic time-scale $t_{chem} = 1/k_1 a_0^n$. If the autocatalytic step itself is fast, the absolute residence-time and decay-times may only be of the order of a few seconds.

Mushrooms, and hence limit cycles, are favoured by large decay times τ_2, i.e. by stable catalysts. This allows the minimum slope of the loss-line, given by $4/\tau_2$, to lie well below the lower tangent. As τ_{res} must exceed τ_2 sustained oscillations will require relatively long residence times.

The ratio of the characteristic times for decay and flow (residence-time) is of particular importance. If the decay is slow, i.e. if $\kappa = k_2/k_{res} = \tau_{res}/\tau_2$ is less than unity, the highest stationary-state for cubic autocatalysis is always stable. If the decay rate is increased with respect to the flow-rate and κ exceeds unity, unstable nodes and foci are possible. The absolute magnitudes of these times are relatively less important.

Higher inlet concentrations γ_0 of the autocatalytic species also favour limit cycles, although very high values lead only to unique solutions. For these conditions ($b_0/a_0 = \gamma_0 \geqq 1/8$) the mushroom-shape of extent of conversion vs residence-time plot "open up", with ignition and extinction being lost along with the regions of hysteresis. The $\gamma_{ss} - \tau_{res}$ curve is tied to zero conversion for $\tau_{res} = 0$ and for $\tau_{res} \to \infty$, rising to a maximum in between, at $\tau_{res} = \tau_2$; the curve is monotonic in τ_{res}. *Critical* slowing-down[7] does not occur; relaxation-times never become infinite, although they do lengthen as the loss-line approaches tangency with the production curve. Critical extinction does occur, see e.g. Fig. 3, and represents the stationary-state reaction rate becoming zero as the flowrate is varied. For the quadratic autocatalysis this is a smooth process, with the reaction rate slowing-down to zero, for cubic autocatalysis there is a discontinuous jump from a finite rate to zero.

By asserting that the Gibbs free energy of a flowing system must attain a minimum, Noyes[8] has argued that under isothermal conditions extinction cannot be achieved by lengthening the residence time and ignition cannot accompany a decrease in t_{res}. The present results refute this conclusion, revealing mushrooms and isolas: it is obvious that G is not constrained to its minimum value in an open reactor in the way that it can be for a closed system.

The existence of a stable limit cycle surrounding a unique unstable focus (Fig. 9c) can be guaranteed. There *may* also be limit cycles for the situations illustrated in Fig. 9(a) and 9(b). In both of these there is a transition from a stable focus to an unstable focus in γ_3 as the dimensionless residence-time is varied. Close to the critical value of τ_{res} there will be a limit cycle in the neighbourhood of γ_3; either on the stable focus side, in which case it will be unstable, or surrounding the unstable focus, in which case it will be stable. Numerical solution of the differential equations may reveal the detailed nature of the phase plane and the existence of limit cycles, in the spirit of Uppal *et al.*[3] or Vaganov *et al.*[4]. Such an investigation will be reported elsewhere.

7. CONCLUSIONS

(1) In a CSTR, "exotic" behaviour patterns such as (i) isolas and mushrooms in plots of conversion vs residence-times and (ii) sustained oscillatory behaviour require neither self-heating nor elaborate kinetic mechanisms: rather elementary autocatalysis under isothermal conditions can suffice.

(2) Two basic schemes demonstrate all the main varieties of behaviour: quadratic or "simple" autocatalysis ($A + B \to 2B$) and cubic autocatalysis ($A + 2B \to 3B$). They are the simplest prototypes of more complicated kinetic structures (possessed, e.g. by large families of enzyme systems and surface catalysis).

(3) The stationary-state behaviour-patterns can be handled algebraically. They can also be illuminated by flow-diagrams. Isola- and mushroom-formation arise in the dependence of extent of reaction upon residence time when catalysis follows the cubic law as soon as the finite lifetime of the catalyst is recognized—most simply, by incorporating its first order decay ($B \to$ inert).

(4) The local stabilities of the stationary states can be determined and the ranges for their occurrence can be evaluated in terms of the rate coefficients and residence time. In the circumstances above, *simple autocatalysis* yields only stable nodal and stable focal behaviour: *cubic autocatalysis* yields the complete range (stable and unstable nodes, saddles, stable and unstable focuses).

(5) Sustained oscillations (limit cycles in the A, B phase plane) are possible for cubic autocatalysis ($n = 2$, $k_2 \neq 0$, $\gamma_0 \neq 0$) over certain ranges of the parameters. These are the simplest circumstances studied so far that give rise to sustained, isothermal oscillatory behaviour.

Acknowledgements— It is a great personal pleasure to be able to acknowledge happy and instructive years spent by P. G. as a junior colleague of Peter Danckwerts in Cambridge from 1951-55.

Our thanks are also due to a referee for a most helpful commentary, and for drawing our attention to the work of Lin[6].

REFERENCES

[1] Gray P., *Ber. Bunsenges. Phys. Chem.* 1980 **84** 309.
[2] Uppal A., Ray W. H. and Poore A. B., *Chem. Engng Sci.* 1974 **29** 967.
[3] Uppal A., Ray W. H. and Poore A. B., *Chem. Engng Sci.* 1976 **31** 205.
[4] Vaganov D. A., Samoilenko N. G. and Abramov V. G., *Chem. Engng Sci.* 1978 **33** 1133.
[5] Kauschus W., Demont J. and Hartmann K., *Chem. Engng Sci.* 1978 **33** 1282.
[6] Lin, K. F., *Can. J. Chem. Engng* 1979 **57** 476; *Chem. Engng Sci.* 1981 **36** 1447.
[7] Heinrichs M. and Schneider F. W., *J. Phys. Chem.* 1981 **85** 2112; *Ber. dts. Bunsenges. Phys. Chem.* 1980 **84** 857.
[8] Noyes R. M., *Proc. Natl. Acad. Sci. U.S.A.* 1981 **78** 7248.
[9] Aarons, L. J. and Gray, B. F., *Chem. Soc. Rev.* 1976 **5** 359.